Biochemical and Biophysical Research Communications 495 (2018) 1167–1174

Contents lists available at ScienceDirect

Biochemical and Biophysical Research Communications

journal homepage: www.elsevier.com/locate/ybbrc

UNC-5 netrin receptor B mediates osteogenic differentiation by modulating bone morphogenetic protein signaling in human adipose-derived stem cells

Xinyi Hu [a, b], Yunsong Liu [a, b], Min Zhang [a, b], Yuejun Wang [a, b], Longwei Lv [a, b], Xiao Zhang [a, b], Ping Zhang [a, b, *], Yongsheng Zhou [a, b]

[a] Department of Prosthodontics, Peking University School and Hospital of Stomatology, Beijing 100081, China
[b] National Engineering Lab for Digital and Material Technology of Stomatology, Peking University School and Hospital of Stomatology, Beijing 100081, China

ARTICLE INFO

Article history:
Received 14 November 2017
Accepted 16 November 2017
Available online 20 November 2017

Keywords:
Osteogenic differentiation
Netrin receptor
Bone morphogenetic protein
Human adipose-derived stem cells
Bone regeneration

ABSTRACT

UNC-5 netrin receptor B (UNC5B) is a dependence receptor of netrin-1 that plays an essential role in mediating angiogenesis and tumorigenesis. Despite its significant roles, there is limited knowledge about the role played by UNC5B in osteogenesis. In the present study, we first demonstrated that UNC5B was required for osteogenic differentiation of human adipose-derived stem cells (hASCs), both in vitro and in vivo. We also found that mechanistically, UNC5B promotes osteogenic differentiation by activating bone morphogenetic protein signaling. These findings point to a new important function of UNC5B and provide a potential basis for hASCs-mediated bone regeneration.

1. Introduction

Bone tissue engineering has been widely studied in the regeneration of bone defects caused by infection, trauma, or tumors [1,2]. Mesenchymal stem cells, including bone marrow-derived mesenchymal stem cells and human adipose-derived stem cells (hASCs), have been demonstrated to be attractive for bone tissue engineering [3,4]. hASCs have received considerable attention in bone tissue engineering because they are easy to harvest, their tissue source is abundant, and they have the potential to differentiate into osteogenic lineages [5–8].

Netrin-1 is a secreted laminin-like matrix protein, initially identified as an axon guidance cue involved in nervous system development and regeneration [9]. It plays a dual role in directing axon pathfinding and neuronal migration via interaction with DCC (Deleted in Colorectal Carcinoma) and UNC5 receptors (UNC5A-D in humans and UNC5H1-4 in rodents) [10]. Netrin-1 is an autocrine factor produced by osteoclast precursors that enhances osteoclast differentiation and function [11], which also promotes atherosclerosis by retaining macrophages in the artery wall [12]. It has recently been proposed to be a multifunctional protein implicated in tumorigenesis, morphogenesis, angiogenesis, inflammation, induced pluripotent stem cell generation, and various pathologies [13–17].

UNC-5 netrin receptor B (UNC5B), the dependent receptor of netrin-1, is a single-pass transmembrane protein that is widely expressed in various embryonic and adult tissues in mammals [18,19]. UNC5B induces apoptosis in the absence of netrin-1, and binding of netrin-1 to UNC5B contributes to protecting embryonic stem cells from apoptosis by restricting UNC5B-mediated apoptosis [17]. Moreover, netrin-1 induces an interaction between UNC5B and the brain-specific GTPase PIKE-L, which hampers UNC5B's proapoptotic activity and enhances neuronal survival by activating PI 3-kinase signaling [20]. UNC5B functions as a negative regulator through inhibiting sprouting angiogenesis [21] and controlling morphogenesis of the vascular system [22]. When activated by Robo4, UNC5B maintains vascular integrity through VEGF signaling in endothelial cells [23]. Further, it has been implicated in tumor suppression in numerous cancers [24]. UNC5B also promotes osteoclast differentiation in the presence of netrin-1, and blockade

Abbreviations: UNC5B, UNC-5 netrin receptor B; hASCs, human adipose-derived stem cells; BMP, bone morphogenetic protein; PM, proliferation medium; OM, osteogenic medium.

* Corresponding author. Department of Prosthodontics, Peking University School and Hospital of Stomatology, 22 Zhongguancun South Avenue, Haidian District, Beijing 100081, China.
E-mail address: zhangping332@bjmu.edu.cn (P. Zhang).

https://doi.org/10.1016/j.bbrc.2017.11.104
0006-291X/

of netrin-1 or UNC5B by antibodies prevents wear particle-induced bone destruction, indicating that UNC5B plays a critical role in inflammatory osteolysis [11,25,26]. However, the role of UNC5B in osteogenic differentiation of hASCs remains unknown.

Bone morphogenetic proteins (BMPs) have been widely studied in the field of bone tissue engineering. Several isotypes of BMPs have been demonstrated to play pleiotropic roles in the osteogenic differentiation of mesenchymal stem cells. Binding of BMPs to transmembrane receptors trigger specific intracellular signaling pathways that control the transcription of specific target genes. The present study was designed to investigate whether UNC5B is involved in the osteogenic differentiation of hASCs and the related mechanisms. We examined whether UNC5B modulates bone morphogenetic protein (BMP) signaling and thereby induces osteogenic differentiation of hASCs. We believe our findings will benefit the development of bone tissue engineering using hASCs.

2. Materials and methods

2.1. Cell culture

hASCs were purchased from ScienCell Research Laboratories (San Diego, CA, USA). They were cultured in proliferation medium (PM) containing DMEM with 10% FBS, 100 U/mL penicillin G, and 100 mg/mL streptomycin. To induce osteogenic differentiation, hASCs were cultured in osteogenic medium (OM) consisting of standard PM with the addition of 10 nM dexamethasone, 10 mM b-glycerophosphate, and 0.2 mM ascorbic acid. All cell-based in vitro experiments were repeated three times.

2.2. Plasmid construction and viral infection

Viral packaging and infection were performed as described previously [27]. Briefly, HEK293T cells at 80% confluency were co-transfected with pLNB vectors containing a mutant CBA promoter for gene expression, short hairpin (sh)RNAs, or plasmids psPAX2 (Clontech, USA) and pVSV-G (Clontech, USA), by using Lipofectamine® 3000 Transfection Reagent (Thermo Fisher Scientific, Rockford, USA). At 36, 48, and 60 h after transfection, the cell supernatant was collected, centrifuged, filtered through an Acrodisc filter with a 0.45-μm PVDF membrane (Pall Corporation, Port Washington, NY, USA), and then precipitated by centrifugation with PEG-it™ (System Biosciences, SBI, Mountain View, CA, USA). hASCs were stably transfected with these lentiviruses at a multiplicity of infection of 100 in the presence of polybrene (5 μg/ml) for 24 h. Stably transfected cells were selected using 1 mg/ml puromycin. The shRNA target sequences were as follows:

UNC5Bsh#1: CTGTCGGACACTGCCAACTAT;
UNC5Bsh#2: GGAGCCGAAACCGCTAATGTT.

2.3. Alkaline phosphatase assays

hASCs were seeded in 6-well plates and 12-well plates. Alkaline phosphatase (ALP) activity was examined after 7 days of osteoinduction. For ALP staining, the NBT/BCIP staining kit (CoWin Biotech, Beijing, China) was used. ALP activity was quantified with an ALP Assay Kit (Nanjing Jiancheng Bioengineering Institute, Nanjing, China). ALP levels were normalized to the total protein content, determined using the BCA method with the Pierce protein assay kit (Thermo Fisher Scientific, Rockford, USA).

2.4. Mineralization assays

Mineralization was determined using alizarin red staining after 14 days of osteoinduction. To quantify matrix calcification, alizarin red was destained with 100 mM cetylpyridinium chloride for 1 h. The absorbance of the released alizarin red was measured at 490 nm and then normalized to total protein content.

2.5. RNA extraction, reverse transcription, and quantitative real-time PCR

Total mRNA was extracted using the Trizol reagent (Invitrogen, Carlsbad, CA, USA) and reverse-transcribed into cDNA using the Reverse Transcription System (Takara, Kusatsu, Japan). Real-time quantitative PCR assays were performed using SYBR Green Master Mix (Life Technologies) on the ABI PRISM 7500 sequence detection system (Applied Biosystems, Foster City, CA, USA). The expression of GAPDH was detected as the internal control. The primer sequences used for the amplification are given in Table 1.

2.6. Western blot

Total protein extraction and western blot were performed as described previously [28]. The primary antibodies used were anti-UNC5B, anti-BMP2, anti-BMP4, and anti-GAPDH (Cell Signaling Technology). The immunoreactive protein bands were visualized using an ECL kit (CWBIO, Beijing, China).

2.7. Bone formation in vivo

hASCs seeded on Bio-Oss Collagen (Geistlich, GEWO, Germany) scaffolds were implanted into the dorsal subcutaneous space of 6-week-old BALB/c nude mice (Peking University Experimental Animal Center). All animal experiments were performed in accordance with the institutional animal guidelines.

Specimens were harvested at 8 weeks after surgery, fixed in 4% paraformaldehyde, decalcified in 10% EDTA, and then embedded in paraffin. Slices were stained with hematoxylin and eosin (H&E), Masson's trichrome, and immunohistochemical staining.

2.8. Statistical analysis

Data were expressed as the mean ± standard deviation (SD). Independent two-tailed Student's *t*-test was used for comparisons between groups. Values of $P < 0.05$ were considered statistically significant. Western blot findings were quantified using the ImageJ software for Windows. All statistical analyses were performed using the GraphPad scientific software for Windows (San Diego, CA, USA).

Table 1
The primer sequences used for quantitative real-time PCR.

Genes	Forward primer (5′-3′)	Reverse (5′-3′)
GAPDH	CGGACCAATACGACCAAATCCG	AGCCACATCGCTCAGACACC
UNC5B	TTACTGGTGCCAGTGCGTGG	TCTTGCGCAGGTAGGCGATG
RUNX2	TCTTAGAACAAATTCTGCCCTTT	TGCTTTGGTCTTGAAATCACA
OCN	AGCAAAGGTGCAGCCTTTGT	GCGCCTGGGTCTCTTCACT
OSX	CCTCCTCAGCTCACCTTCTC	GTTGGGAGCCCAAATAGAAA
COL1A1	TGGTCCCAAGGGTAACAGCG	AACACCAACAGGGCCAGGCT

3. Results

3.1. Endogenous expression of UNC5B is significantly downregulated in hASCs undergoing osteogenic differentiation

In order to investigate the involvement of UNC5B in osteogenesis, its expression profile in hASCs was examined. As shown in Fig. 1A–C, RT-qPCR showed that *UNC5B* expression was significantly downregulated ($P < 0.001$) during the osteogenic differentiation of hASCs, and this was accompanied by stimulation of the osteogenic marker genes *RUNX2* and *OCN*. In addition, the level of *UNC5B* was selectively decreased in hASCs after osteogenic induction and was negatively correlated with *RUNX2* levels (Fig. 1D and E).

3.2. Inhibition of UNC5B significantly impairs osteogenic differentiation of hASCs in vitro

To further confirm whether UNC5B plays a critical role in the osteogenic differentiation of hASCs, we established stable *UNC5B*-knockdown cells using lentivirus expressing *UNC5B* shRNA. As shown in Fig. 2A–D, the knockdown efficiency was >80% as determined by fluorescent staining, RT-qPCR, and western blotting. After the hASCs were cultured in OM for 7 days, the ALP activity decreased significantly with *UNC5B* knockdown ($P < 0.001$), as determined from ALP staining and quantification (Fig. 2E and F). Moreover, alizarin red S staining and quantification showed that extracellular matrix mineralization was impaired in *UNC5B*-knockdown cells (Fig. 2G and H). To further confirm the important role of UNC5B in osteogenic differentiation, we examined the mRNA expression of several osteogenic markers in both control and *UNC5B*-silenced cells. After 14 days of osteoinduction, *UNC5B* knockdown significantly inhibited ($P < 0.001$) the expressions of *RUNX2* and *OSX* (Fig. 2I and J). To rule out the off-target effect, we established *UNC5B*-knockdown cells with another independent *UNC5B* shRNA fragment (Figs. S1A–C). As shown in Supplemental Figs. 1D–H, osteogenic differentiation was also blocked in *UNC5B*-knockdown cells. Taken together, the results suggest that *UNC5B*

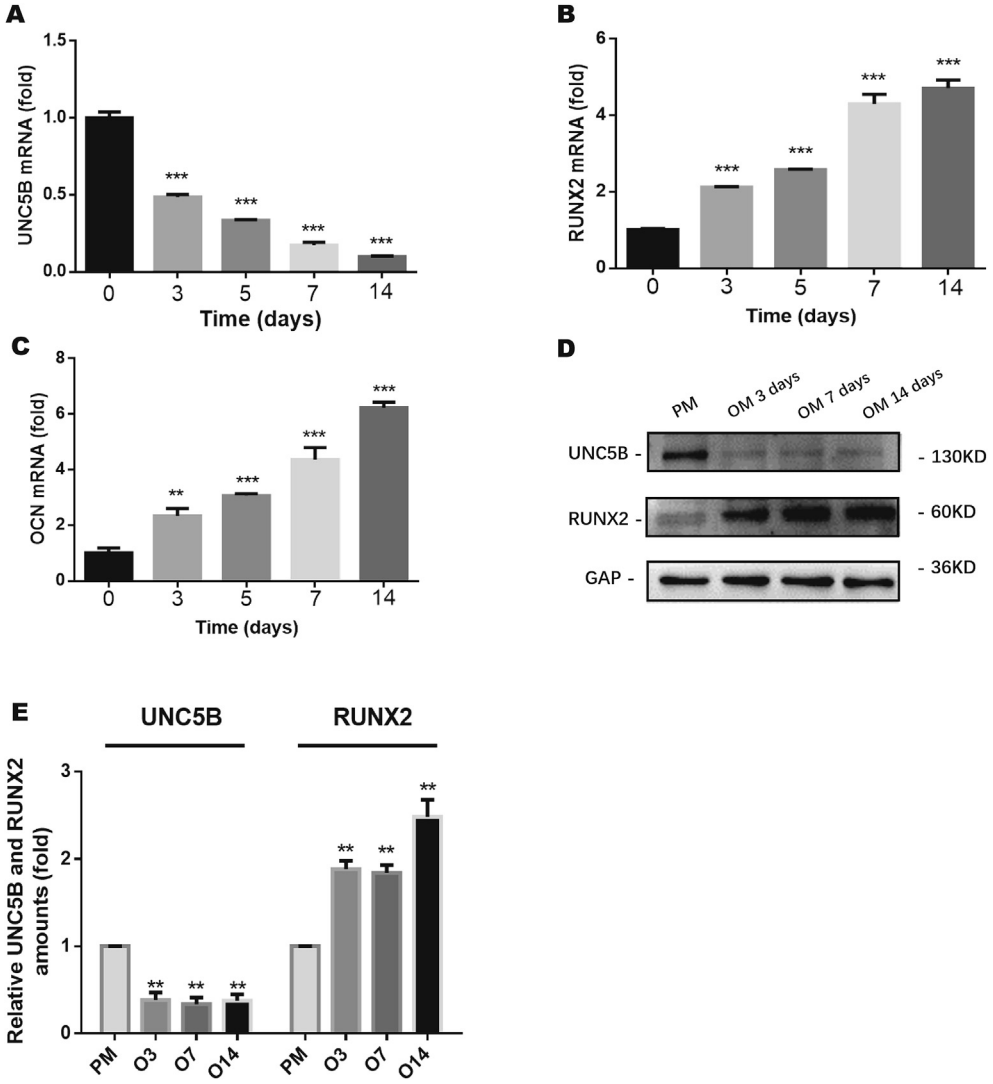

Fig. 1. Expression of endogenous *UNC5B* during osteogenic induction in hASCs.
(A–C) Quantitative real-time PCR analysis of *UNC5B* (A), *RUNX2* (B), and *OCN* (C) expression in hASCs after 3, 5, 7, and 14 days of osteogenic induction.
(D, E) Western blotting (D) and quantification (E) of *UNC5B* and RUNX2 expression in hASCs after 3, 7, and 14 days of osteogenic induction.
All data are shown as the mean ± SD, n = 3. ***$P < 0.001$, **$P < 0.01$ versus the control group. PM = proliferation medium; OM = osteogenic medium; O3 = incubation in OM for 3 days; O7 = incubation in OM for 7 days; O14 = incubation in OM for 14 days.

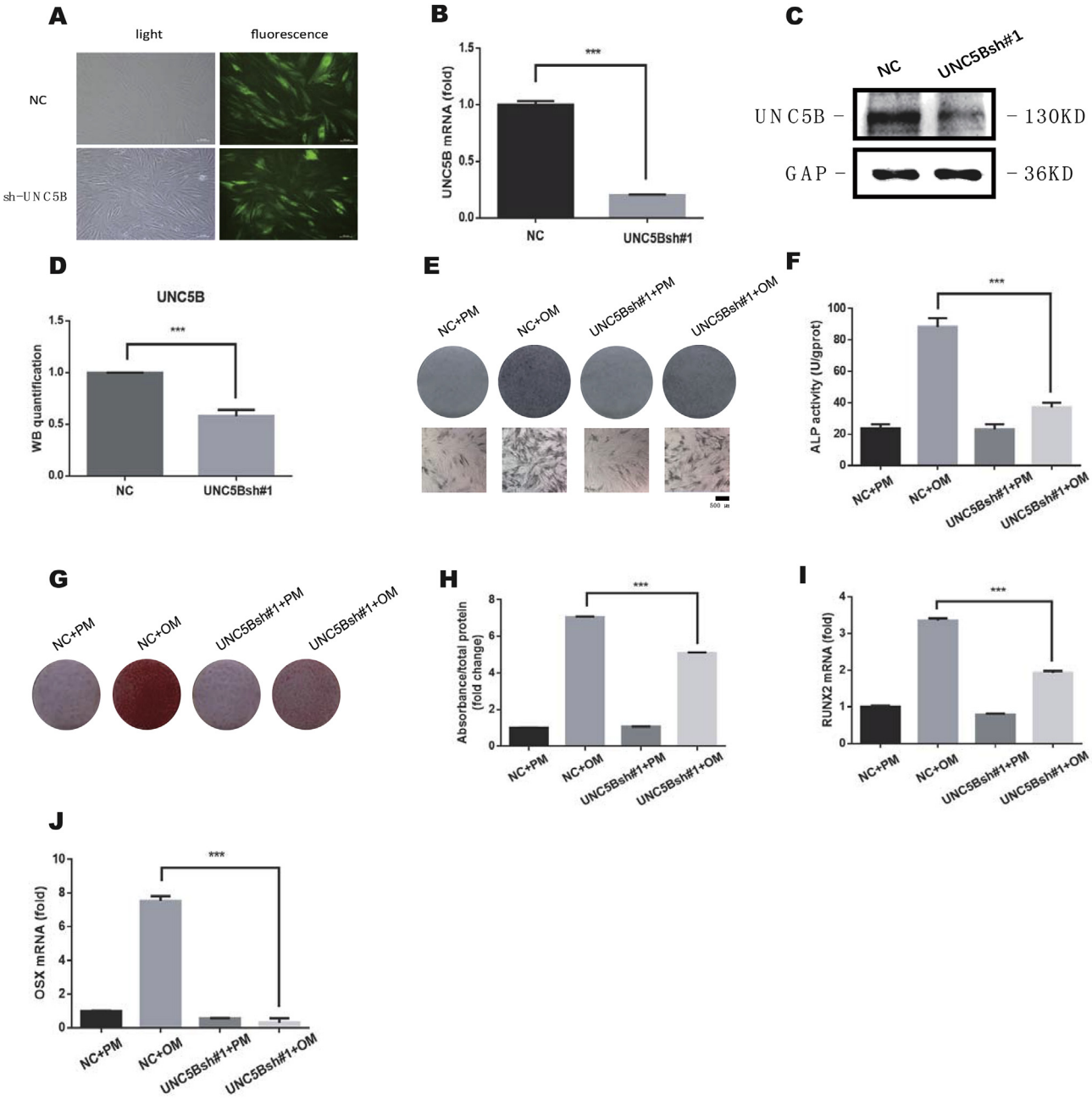

Fig. 2. Knockdown of *UNC5B* inhibits osteogenic differentiation in vitro.
(A) Microscopic images of GFP-positive hASCs under ordinary and fluorescent light. Scale bar, 100 μm.
(B–D) Knockdown of *UNC5B* was validated by quantitative real-time PCR (B) and western blotting (C, D).
(E, F) Knockdown of *UNC5B* decreased ALP activity in hASCs. Control or *UNC5B*-knockdown cells were treated with proliferation or osteogenic media for 7 days for ALP staining (E) and quantification (F). Scale bar, 500 μm.
(G, H) Knockdown of *UNC5B* impaired mineralization in hASCs. Control or *UNC5B* knockdown cells were treated with proliferation or osteogenic media for 14 days for ARS staining (G) and quantification (H).
(I, J) Quantitative real-time PCR analysis of *RUNX2* (I) and *OSX* (J) expression in transfected hASCs.
All data are shown as the mean ± SD, n = 3. ***$P < 0.001$. PM = proliferation medium; OM = osteogenic medium; NC = control cells; UNC5Bsh = *UNC5B*-knockdown cells; WB = western blotting; GAP = glyceraldehyde phosphate dehydrogenase; ALP = alkaline phosphatase.

knockdown inhibits osteogenic differentiation in vitro.

3.3. UNC5B knockdown inhibits the osteogenic differentiation of hASCs in vivo

To verify our in vitro findings, we examined whether *UNC5B* knockdown affected hASC-mediated bone formation in vivo. Control or *UNC5B*-knockdown cells were seeded on Bio-Oss Collagen scaffolds separately and then transplanted into nude mice. Transplants were harvested and subjected to histological analysis after 8 weeks. H&E and Masson's trichrome staining showed that the *UNC5B*-knockdown cells formed less bone tissue than the control cells did, as shown in Fig. 3A and B. Moreover, the size and intensity of osteoblasts and bone trabeculae positive for

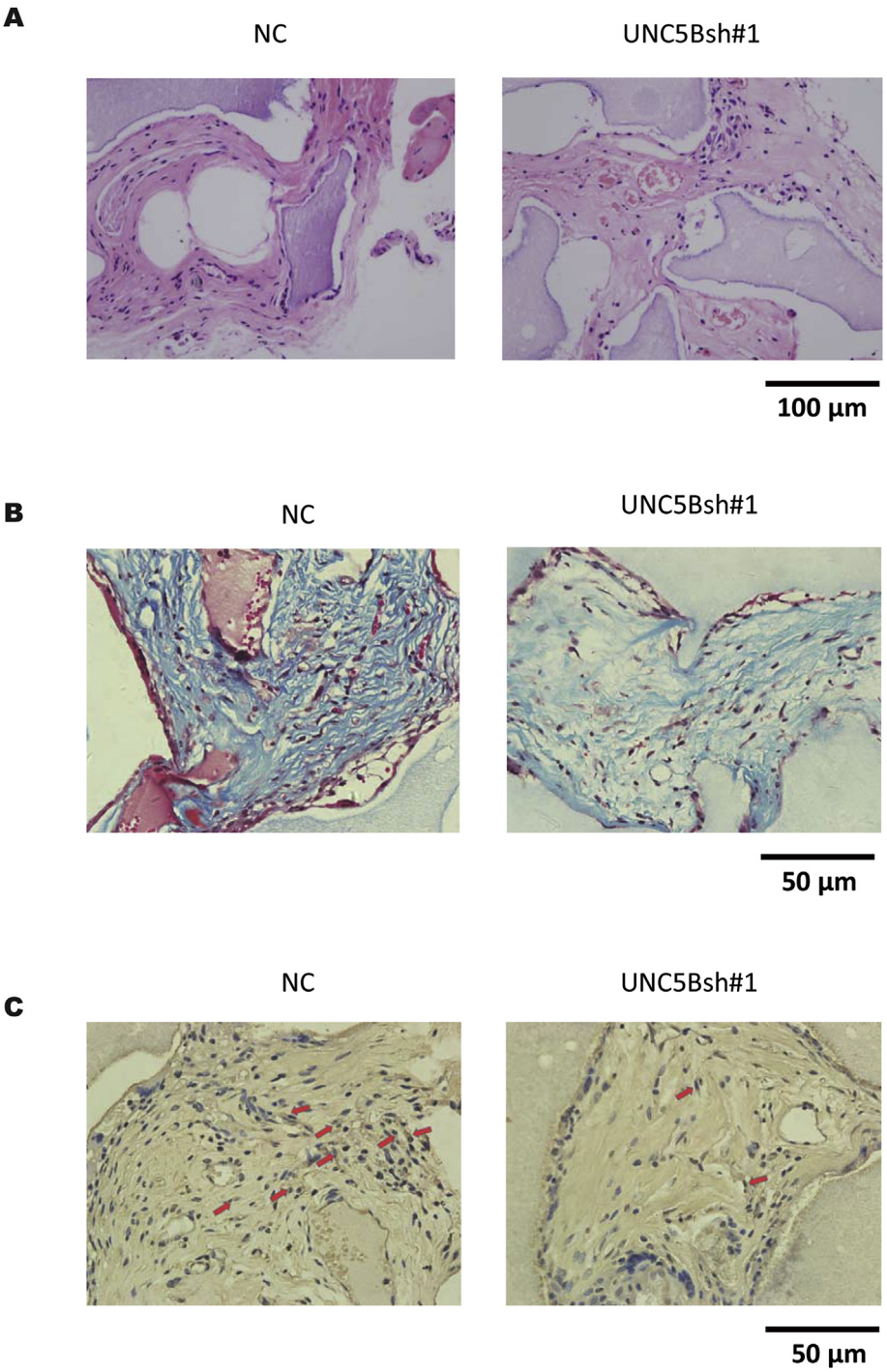

Fig. 3. Knockdown of *UNC5B* inhibits osteogenic differentiation in vivo.
(A) *UNC5B* knockdown reduced bone formation in vivo, as determined by H&E staining of histological sections from implanted hASCs-scaffold hybrids.
(B) Masson's trichrome staining of histological sections from implanted hASCs-scaffold hybrids.
(C) Immunohistochemical staining for OCN. Dark-brown granules indicating positive staining are marked by blue arrows.
Scale bar, 100 μm in (A) and 50 μm in (B) and (C). OCN = osteocalcin.

OCN observed on immunohistochemical staining (Fig. 3C) were significantly lower in the *UNC5B*-knockdown cells than those in the control cells.

3.4. UNC5B positively regulates BMP signaling

It has been demonstrated that netrin-1 and its receptor promote the migration of RSC96 cells by activating p38 MAPK and PI3K-Akt signal cascades [29]. To further explore the molecular mechanisms by which UNC5B regulates the osteogenic differentiation of hASCs, we performed western blot analysis to compare the protein levels of p-p38 and p-Akt between *UNC5B*-knockdown and control cells. However, we did not find significant MAPK or Akt signal changes in *UNC5B*-silenced cells (SFig. 2A and B).

Next, we performed RT-qPCR analysis to screen the expression of key genes associated with osteogenic differentiation in hASCs. Interestingly, we found that mRNA expression of *BMP2*, *BMPR1A*, and *BMPR1B* were significantly decreased ($P < 0.001$) in *UNC5B*-knockdown cells, as shown in Fig. 4A. In addition, *UNC5B* knockdown with another shRNAs also led to a reduction in the expression of a subset of BMP signaling genes (SFig. 2E). Further, western blotting and quantification of the electrophoresis bands showed

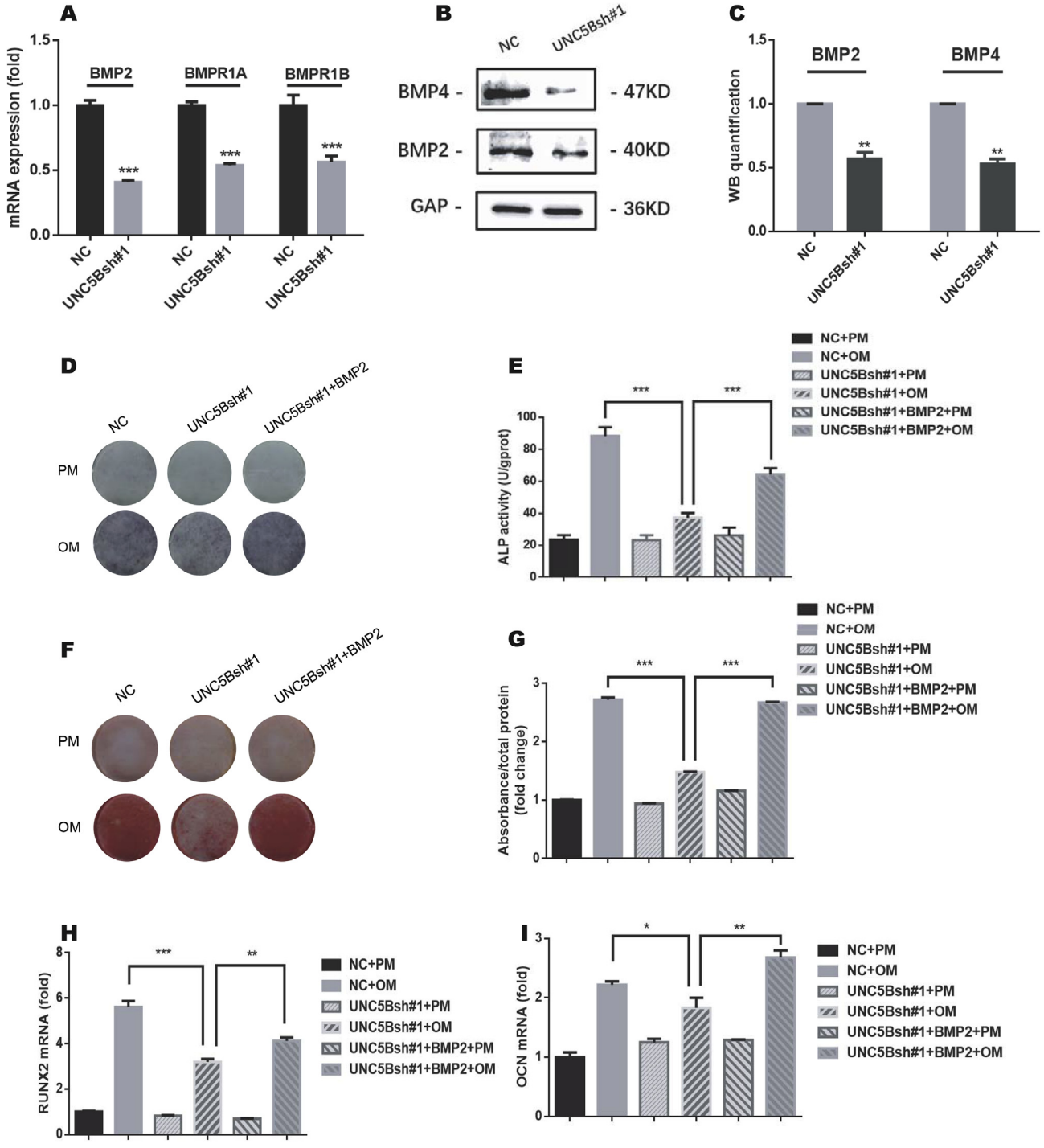

Fig. 4. *UNC5B* regulates osteogenic differentiation through the BMP signaling pathway.
(A) Quantitative real-time PCR analysis of *BMP2*, *BMPR1A*, and *BMPR1B* expression in transfected hASCs.
(B, C) Western blotting (B) and quantification (C) of *BMP2* and *BMP4* expression in transfected hASCs.
(D, E) Control or *UNC5B*-knockdown cells were treated with BMP2 (200 ng/ml), which reversed the decrease in ALP staining (D) and quantification (E) brought about by *UNC5B* knockdown.
(F, G) Control or *UNC5B*-knockdown cells were treated with BMP2 (200 ng/ml), which reversed the decrease in ARS staining (F) and quantification (G).
(H, I) BMP2 treatment promoted the expression of *OCN* (H) and *RUNX2* (I) in *UNC5B*-knockdown cells as determined by quantitative real-time PCR.
All data are shown as the mean ± SD, n = 3. $^{***}P < 0.001$, $^{**}P < 0.01$, $^{*}P < 0.05$.

that downregulation of *UNC5B* could suppress BMP2/4 expression at the protein level (Fig. 4B and C & SFig. 2C and D). To further determine the functional connection between UNC5B and BMP signaling in osteogenic differentiation, we examined the effect of *BMP2* on osteogenesis in *UNC5B*-knockdown cells. As shown in Fig. 4D–G and SFig. 2F–I, treatment of *UNC5B*-knockdown cells with BMP2 reversed the decrease in ALP activity and extracellular matrix mineralization. Moreover, the downregulation of *RUNX2* and *OCN* expression was reversed by BMP2 treatment (Fig. 4H and I and SFig. 2J and K). Collectively, our data suggest that UNC5B regulates osteogenic differentiation through the BMP signaling pathway.

4. Discussion

In the present study, we demonstrated the important function of UNC5B during the osteogenesis of hASCs. Moreover, in our mechanical study, we identified a novel connection between UNC5B and the BMP pathway.

We first established stable *UNC5B*-knockdown cells and confirmed that *UNC5B* knockdown inhibited the osteogenic capacity of hASCs in vitro, as determined on the basis of ALP activity, matrix mineralization assays, and osteogenic gene expression profiles. The role played by UNC5B in osteogenesis in vivo was also confirmed by subcutaneous transplantation in the dorsa of nude mice. These results suggested that downregulation of *UNC5B* could inhibit the osteogenic differentiation of hASCs.

Further, we found that UNC5B was a positive regulator of BMP signaling, which was shown to play diverse roles in osteogenesis. BMP2 could significantly promote osteogenic differentiation of hASCs [30–32]. The mRNA expression of several BMP signaling genes was hampered in *UNC5B*-knockdown cells. Moreover, *UNC5B* downregulation suppressed BMP2/4 expression at the protein level. Treatment of *UNC5B*-knockdown cells with BMP2 reversed the inhibition of the osteogenic capacity of hASCs in vitro. Collectively, our study indicated that UNC5B regulates osteogenic differentiation through the BMP signaling pathway.

It is noteworthy that while UNC5B expression was significantly decreased upon osteogenic induction, UNC5B played a positive role in osteogenesis of hASCs. It is reasonable to postulate that UNC5B is degraded after promoting osteogenic differentiation in the early stage to prevent osteopetrosis. As is well known, bone homeostasis is regulated by bone formation and resorption through osteoblasts and osteoclasts [33]. Osteopetrosis is a heritable disease of increased bone mass and density caused by abnormal osteoclast with defective ruffled-border formation [33–35]. Protein degradation can be achieved through the autophagy and ubiquitin-proteasome pathways, both of which were reported to play critical roles in osteogenesis. Autophagy is a lysosomal degradation pathway responsible for the degradation and recycling of cellular components such as unnecessary organelles and proteins [36,37], and recent evidence suggests that autophagy plays an important role in the maintenance of bone homeostasis [38]. Further investigation may be necessary to examine whether UNC5B was downregulated by autophagy-triggered degradation. In the ubiquitin-proteasome pathway, proteins are first tagged by multiple ubiquitin molecules, after which the polyubiquitinated proteins are degraded to small peptides by the 26S proteasome complex [39]. It is reported that β-catenin and Runx2 are regulated by the ubiquitin-proteasome pathway [40,41]. Proteasome inhibitors (PIs) induce osteoblast differentiation by activating the β-catenin/TCF pathway and increasing Runx2 activity [42,43]. Moreover, PIs suppress osteoclastogenesis by inhibiting RANKL-induced NF-kB activation [44]. Further studies are required to determine the mechanism underlying a decrease in UNC5B during osteogenic induction.

Our findings confirm that UNC5B is a potential target for osteogenic commitment of hASCs. This novel role played by UNC5B may provide valuable information for bone tissue engineering and cell-based therapies for bone defects.

Acknowledgements

This study was supported by grants from the National Natural Science Foundation of China (No. 81570953 to Y.Z., No. 81500822 to P.Z.), the Project for Culturing Leading Talents in Scientific and Technological Innovation of Beijing (Z171100001117169 to Y.Z.), the PKU School of Stomatology for Talented Young Investigators (PKUSS20140109 to P.Z.), and the Construction Program for National Key Clinical Specialty from National Health and Family Planning Commission of China (2011 to Y.Z.).

Appendix A. Supplementary data

Supplementary data related to this article can be found at https://doi.org/10.1016/j.bbrc.2017.11.104.

Transparency document

Transparency document related to this article can be found online at https://doi.org/10.1016/j.bbrc.2017.11.104.

References

[1] P. Bianco, P.G. Robey, Stem cells in tissue engineering, Nature 414 (2001) 118–121.
[2] H. Petite, V. Viateau, W. Bensaïd, et al., Tissue-engineered bone regeneration, Nat. Biotechnol. 18 (2000) 959–963.
[3] I. Sekiya, B.L. Larson, J.R. Smith, et al., Expansion of human adult stem cells from bone marrow stroma: conditions that maximize the yields of early progenitors and evaluate their quality, Stem Cells 20 (2002) 530–541.
[4] B. Parekkadan, J.M. Milwid, Mesenchymal stem cells as therapeutics, Annu. Rev. Biomed. Eng. 12 (2010) 87–117.
[5] M. Barba, et al., Adipose-derived mesenchymal cells for bone regereneration: state of the art, BioMed Res. Int. 2013 (2013) 1–11.
[6] M. Locke, V. Feisst, P.R. Dunbar, Concise review: human adipose-derived stem cells: separating promise from clinical need, Stem Cells 29 (3) (2011) 404–411.
[7] B. Levi, M.T. Longaker, Concise review: adipose-derived stromal cells for skeletal regenerative medicine, Stem Cells 29 (4) (2011) 576–582.
[8] D.S. Han, et al., Consideration of bone regeneration effect of stem cells, J. Craniofac. Surg. 25 (1) (2014) 196–201.
[9] P. Mehlen, C. Furne, Netrin-1: when a neuronal guidance cue turns out to be a regulator of tumorigenesis, Cell. Mol. Life Sci. 62 (22) (2005) 2599–2616.
[10] K. Hong, et al., A ligand-gated association between cytoplasmic domains of UNC5 and DCC family receptors converts netrin-induced growth cone attraction to repulsion, Cell 97 (7) (1999) 927–941.
[11] A. Mediero, et al., Netrin-1 is a critical autocrine/paracrine factor for osteoclast differentiation, J. Bone Min. Res. 30 (5) (2015) 837–854.
[12] J.M. van Gils, et al., The neuroimmune guidance cue netrin-1 promotes atherosclerosis by inhibiting the emigration of macrophages from plaques, Nat. Immunol. 13 (2) (2012) 136–143.
[13] P. Mehlen, C.L. Delloye-Bourgeois, A. Ch Dotal, Novel roles for Slits and netrins: axon guidance cues as anticancer targets? Nat. Rev. Cancer 11 (3) (2011) 188–197.
[14] V. Cirulli, M. Yebra, Netrins: beyond the brain, Nat. Rev. Mol. Cell Biol. 8 (4) (2007) 296–306.
[15] B. Larrivee, et al., Activation of the UNC5B receptor by Netrin-1 inhibits sprouting angiogenesis, Genes Dev. 21 (19) (2007) 2433–2447.
[16] A. Mediero, et al., Netrin-1 is highly expressed and required in inflammatory infiltrates in wear particle-induced osteolysis, Ann. Rheum. Dis. 75 (9) (2016) 1706–1713.
[17] D. Ozmadenci, et al., Netrin-1 regulates somatic cell reprogramming and pluripotency maintenance, Nat. Commun. 6 (2015) 7398.
[18] K. Hata, et al., Unc5B associates with LARG to mediate the action of repulsive guidance molecule, J. Cell Biol. 184 (5) (2009) 737–750.
[19] R. Wang, et al., Autoinhibition of UNC5b revealed by the cytoplasmic domain structure of the receptor, Mol. Cell 33 (6) (2009) 692–703.
[20] X. Tang, et al., Netrin-1 mediates neuronal survival through PIKE-L interaction with the dependence receptor UNC5B, Nat. Cell Biol. 10 (6) (2008) 698–706.
[21] B. Larrivee, et al., Activation of the UNC5B receptor by Netrin-1 inhibits

sprouting angiogenesis, Genes Dev. 21 (19) (2007) 2433–2447.
[22] X Lu, et al., The netrin receptor UNC5B mediates guidance events controlling morphogenesis of the vascular system, Nature 432 (2004) 179–186.
[23] A.W. Koch, et al., Robo4 maintains vessel integrity and inhibits angiogenesis by interacting with UNC5B, Dev. Cell 20 (1) (2011) 33–46.
[24] H. Arakawa, Netrin-1 and its receptors in tumorigenesis, Nat. Rev. Cancer 4 (12) (2004) 978–987.
[25] A. Mediero, et al., Netrin-1 and its receptor Unc5b are novel targets for the treatment of inflammatory arthritis, FASEB J. 30 (2016) 3835–3844.
[26] A. Mediero, et al., Netrin-1 is highly expressed and required in inflammatory infiltrates in wear particle-induced osteolysis, Ann. Rheum. Dis. 75 (9) (2016) 1706–1713.
[27] P. Zhang, et al., Histone acetyltransferase GCN5 regulates osteogenic differentiation of mesenchymal stem cells by inhibiting NF-κB, J. Bone Mineral Res. 31 (2) (2016) 391–402.
[28] P. Zhang, et al., Tumor suppressor p53 cooperates with SIRT6 to regulate gluconeogenesis by promoting FoxO1 nuclear exclusion, Proc. Natl. Acad. Sci. 111 (29) (2014) 10684–10689.
[29] J. Lv, et al., Netrin-1 induces the migration of Schwann cells via p38 MAPK and PI3K-Akt signaling pathway mediated by the UNC5B receptor, Biochem. Biophys. Res. Commun. 464 (1) (2015) 263–268.
[30] X. Zhang, et al., The roles of bone morphogenetic proteins and their signaling in the osteogenesis of adipose-derived stem cells, Tissue Eng. Part B Rev. 20 (1) (2014) 84–92.
[31] C. Kaps, et al., Distinct roles of BMP receptors Type IA and IB in osteo-/chondrogenic differentiation in mesenchymal progenitors (C3H10T1/2), Biofactors 20 (2) (2004) 71–84.
[32] X. Zhang, et al., Effects of heterodimeric bone morphogenetic protein-2/7 on osteogenesis of human adipose-derived stem cells, Cell Prolif. 48 (6) (2015) 650–660.
[33] I.M. Shapiro, et al., Boning up on autophagy, Autophagy 10 (1) (2013) 7–19.
[34] C. Sobacchi, et al., Osteopetrosis: genetics, treatment and new insights into osteoclast function, Nat. Rev. Endocrinol. 9 (9) (2013) 522–536.
[35] J. Tolar, S.L. Teitelbaum, P.J. Orchard, Osteopetrosis, N. Engl. J. Med. 351 (27) (2004) 2839–2849.
[36] V. Pierrefite-Carle, et al., Autophagy in bone: self-eating to stay in balance, Ageing Res. Rev. 24 (2015) 206–217.
[37] B. Levine, D.J. Klionsky, Development by self-digestion: molecular mechanisms and biological functions of autophagy, Dev. Cell 6 (4) (2004) 463–477.
[38] C. Greenhill, Bone: autophagy regulates bone growth in mice, Nat. Rev. Endocrinol. 12 (1) (2015) 4.
[39] M.H. Glickman, A. Ciechanover, The ubiquitin-proteasome proteolytic pathway: destruction for the sake of construction, Physiol. Rev. 82 (2) (2002) 373–428.
[40] H. Aberle, et al., beta-catenin is a target for the ubiquitin-proteasome pathway, EMBO J. 16 (13) (1997) 3797–3804.
[41] M. Zhao, et al., E3 ubiquitin ligase Smurf1 mediates core-binding factor alpha1/Runx2 degradation and plays a specific role in osteoblast differentiation, J. Biol. Chem. 278 (30) (2003) 27939–27944.
[42] Y.W. Qiang, et al., Bortezomib induces osteoblast differentiation via Wnt-independent activation of beta-catenin/TCF signaling, Blood 113 (18) (2009) 4319–4330.
[43] Y. Qiang, et al., Proteasome inhibitors and bone disease, Seminars Hematol. 49 (3) (2012) 243–248.
[44] I. von Metzler, et al., Bortezomib inhibits human osteoclastogenesis, Leukemia 21 (9) (2007) 2025–2034.